Pet. Sci. (2015) 12:470–482
DOI 10.1007/s12182-015-0033-x

ORIGINAL PAPER

An experimental and numerical study of chemically enhanced water alternating gas injection

Saeed Majidaie[1] · Mustafa Onur[2] · Isa M. Tan[3]

Received: 27 October 2014 / Published online: 9 July 2015

Abstract In this work, an experimental study combined with numerical simulation was conducted to investigate the potential of chemically enhanced water alternating gas (CWAG) injection as a new enhanced oil recovery method. The unique feature of this new method is that it uses alkaline, surfactant, and polymer additives as a chemical slug which is injected during the water alternating gas (WAG) process to reduce the interfacial tension (IFT) and simultaneously improve the mobility ratio. In essence, the proposed CWAG process involves a combination of chemical flooding and immiscible carbon dioxide (CO_2) injection and helps in IFT reduction, water blocking reduction, mobility control, oil swelling, and oil viscosity reduction due to CO_2 dissolution. Its performance was compared with the conventional immiscible water alternating gas (I-WAG) flooding. Oil recovery utilizing CWAG was better by 26 % of the remaining oil in place after waterflooding compared to the recovery using WAG conducted under similar conditions. The coreflood data (cumulative oil and water production) were history matched via a commercial simulator by adjusting the relative permeability curves and assigning the values of the rock and fluid properties such as porosity, permeability, and the experimentally determined IFT data. History matching of the coreflood model helped us optimize the experiments and was useful in determining the importance of the parameters influencing sweep efficiency in the CWAG process. The effectiveness of the CWAG process in providing enhancement of displacement efficiency is evident in the oil recovery and pressure response observed in the coreflood. The results of sensitivity analysis on CWAG slug patterns show that the alkaline–surfactant–polymer injection is more beneficial after CO_2 slug injection due to oil swelling and viscosity reduction. The CO_2 slug size analysis shows that there is an optimum CO_2 slug size, around 25 % pore volume which leads to a maximum oil recovery in the CWAG process. This study shows that the ultralow IFT system, i.e., IFT equaling 10^{-2} or 10^{-3} mN/m, is a very important parameter in CWAG process since the water blocking effect can be minimized.

Keywords Enhanced water alternating gas (CWAG) · Enhanced oil recovery · Interfacial tension · Mobility control · Water blocking

1 Introduction

The immiscible CO_2 flooding process holds promise for incremental recovery from reservoirs with low to moderate pressures, where it is difficult to attain the minimum miscibility pressure (MMP) of the reservoir fluid. CO_2 gas injection is more desirable compared to other injection gases due to its lower injectivity problems, lower formation volume factor, abundance of reserves, and higher incremental oil recovery (Kulkarni 2003; Al-Abri and Amin 2010). The microscopic sweep efficiency of CO_2 injection is good; however, the mobility ratio which controls the volumetric sweep efficiency between CO_2 and oil is poor

✉ Saeed Majidaie
saeedan8@gmail.com; saeed.majidaie@leap-energy.com

[1] Leap Energy- Subsurface Consulting Services, Kuala Lumpur, Malaysia

[2] Department of Petroleum and Natural Gas Engineering, Istanbul Technical University, Istanbul, Turkey

[3] Applied Science Department, Universiti Teknologi Petronas, Tronoh, Perak, Malaysia

Edited by Yan-Hua Sun

(Hinderaker et al. 1996; Faisal et al. 2009). Most of the CO_2 field projects have experienced early gas breakthrough at the producers (Martin et al. 1988).

Caudle and Dyes (1958) noticed that the sweep efficiency of a gas injection process can be increased by decreasing the mobility behind the flooding front. This is achieved by injecting a water slug along with the gas slug. The water slug can reduce the relative permeability to gas and therefore lower the total mobility. In their proposed method, a miscible slug is driven by a simultaneous injection of water and gas in a proper ratio. To avoid injectivity problems and other operational limitations related to the simultaneous fluid injection, an injection scheme involving the alternate injection of gas and water, water alternating gas (WAG), is used.

However, recent studies show that most of the fields could not reach the expected recovery from a WAG process (Sharma and Rao 2008). The average recovery in miscible and immiscible WAG was 9.7 % and 6.4 % of the original oil in place (OOIP), respectively (Christensen et al. 2001). Some studies have reviewed the main issues associated with a WAG process. The main issues are water blocking phenomena and WAG mobility control (Kulkarni 2003; Rao et al. 2004).

The injected water can isolate the residual oil from contact with gas. Due to the high interfacial tension (IFT) between water and oil, it is not possible for water to remove the trapped oil from the pores. This phenomenon is known as the water blocking effect and it reduces the displacement efficiency at the pore scale (Green and Willhite 1998; Muller and Lake 1991). Water blocking is a strong function of rock wettability and more detrimental in water-wet rocks (Lin and Huang 1990).

In highly viscous oil reservoirs, the injected water has a low viscosity compared to the reservoir oil which makes an unstable front behind the oil bank. Viscous fingering of injected water causes the injected gas to have higher mobility and early breakthrough which bypasses many portions of the reservoir. In this condition, the WAG mobility ratio becomes unfavorable (Tchelepi and Orr 1994; Dehghan et al. 2010).

To overcome the aforementioned issues and improve the efficiency of conventional WAG process, a new EOR method, which will be referred to as the chemically enhanced WAG (CWAG) in this paper, is proposed. In this CWAG method, alkali, surfactant, and polymer are injected as a chemical slug during the WAG process to minimize the water blocking effect by IFT reduction and to improve the mobility ratio using the polymer. The CWAG process includes a chemical slug which is preceded by CO_2 and followed by water, and followed by alternate CO_2 and water slugs. In another practice, a chemical slug is injected after one cycle of gas and water slugs and is followed by water and gas alternating slugs. This new method combines the features of immiscible CO_2 flooding with the alkali-surfactant-polymer (ASP) and improves the efficiency of the current WAG treatment.

Alkaline and surfactant additives are typical in a chemical flooding which can reduce IFT significantly. Alkaline additives can react with the acidic components of crude oil to generate in situ surfactants or soap. The combination of the soap and surfactant can reduce the IFT to ultralow values such as 10^{-2} or 10^{-3} mN/m. By having an ultralow IFT from alkaline–surfactant system, it is possible to minimize the effect of water blocking in the WAG process. WAG mobility control can be further enhanced using polymer to increase the aqueous phase viscosity. Therefore, mobility control which is a concern for high-viscosity oil can be improved by CWAG process.

In this study, our objective is to demonstrate the EOR potential of the CWAG process both experimentally and numerically. The performance of the CWAG process is compared with that of the conventional WAG flooding. The coreflood data (cumulative oil and water production) are history-matched via a commercial simulator by adjusting the relative permeability curves and assigning the values of the rock and fluid properties such as porosity, permeability, and experimentally determined IFT data. History matching of the coreflood model was instrumental in optimizing the experiments and in evaluating the criticality of the parameters that influence sweep efficiency in the CWAG process.

2 Experimental description

2.1 Materials

The main chemicals used in this study are surfactants, alkali, and polymer. The chemicals selected were 1 wt% NaCl brine and crude oil during phase behavior and coreflood experiments. Pure CO_2 (99.99 % purity) was used during CWAG and WAG floodings. The crude oil used for phase behavior and coreflood experiments had a viscosity of 1.6 cP and a density of 0.8 g/cm^3 at 85 °C, respectively. The acid value of the crude oil was 0.37 mg KOH/g oil. 1 wt% NaCl was used during saturation, brine injection, waterflooding, WAG, and CWAG.

Three available surfactants named as Petrostep S13A, S3B, and S13C were tested in phase behavior experiments. Sodium carbonate (Na_2CO_3) is a conventional alkali, and offers the additional advantage of speeding microemulsion equilibration, resulting in quick mobilization of residual oil. Polymer SNF-3330S is the most extensively used polymer in coreflood experiments. It had a molecular weight of approximately 8 million Daltons and a degree of hydrolysis of 30 %.

2.2 Experimental procedures

Chemical additives (i.e., surfactant, alkali, polymer, and electrolyte) are evaluated based on their microemulsion phase behavior. As is well known, a microemulsion is a thermodynamically stable and clear dispersion of oil and water, in combination with surfactant molecules (Ruckenstein 1981; Walker et al. 2012). Winsor (1985) identified that for a microemulsion system with a fixed surfactant concentration, selected crude oil, and different salinity, the phase behavior of microemulsion can be classified into three different classes: microemulsion Type I (or lower phase microemulsion), microemulsion Type II (or upper phase microemulsion), and microemulsion Type III (or middle phase microemulsion). Microemulsion Type III is formed in equilibrium with both excess oil and brine. Because of high solubilization ratio and ultralow IFT between Type III and crude oil/aqueous interfaces, this type of microemulsion is of great interest in the EOR process.

Microemulsion phase behavior was investigated by mixing aqueous surfactant solution, electrolytes with different salinities, and/or alkali with oil at a specific water/oil ratio (1:1) in glass vials or pipettes. They were first shaken well by hand for 1 min, and then aged in an oven at 85 °C. The solubilization parameters of water and oil are defined as the ratio of the volume of the respective phase solubilized by the microemulsion phase to the volume of surfactant present in the microemulsion phase. It is assumed for this calculation that all of the surfactants are contained in the microemulsion phase. At optimum salinity, where microemulsion Type III is present, the amount of oil and brine solubilized into the microemulsion phase is approximately equal. The intersection of oil and water solubilization ratio curves is defined as the optimal solubilization ratio and optimal salinity (e.g. refer to Fig. 7). A high oil and water solubilization ratio at optimal salinity is correlated with an ultralow IFT, which is the key mechanism in surfactant-based chemical EOR. The details of this method are well established (Flaaten et al. 2009; Liu et al. 2010; Levitt et al. 2011). Determining the IFT value at optimal salinity is very important in surfactant selection and performance. Huh (1979) derived a theoretical relationship between solubilization ratio and IFT at optimum salinity:

$$\sigma = \frac{0.3}{(V_i/V_s)^2}, \tag{1}$$

where σ is IFT, V_i is the oil/water volume present in the microemulsion, and V_s is the total surfactant volume present in the test tube. Huh's equation (Eq. 1) has been found to give a good estimate of the IFT over a wide range of salinity and other variables for a large number of crude oils.

The selected chemical formulation was used in conjugation with WAG injection in CWAG coreflood experiments for good oil recovery and low pressure gradient using Berea sandstone cores saturated with saline brine at residual oil saturation. Figure 1 shows a schematic of a coreflood setup for performing WAG or CWAG tests. The coreflood data were analyzed to identify the various

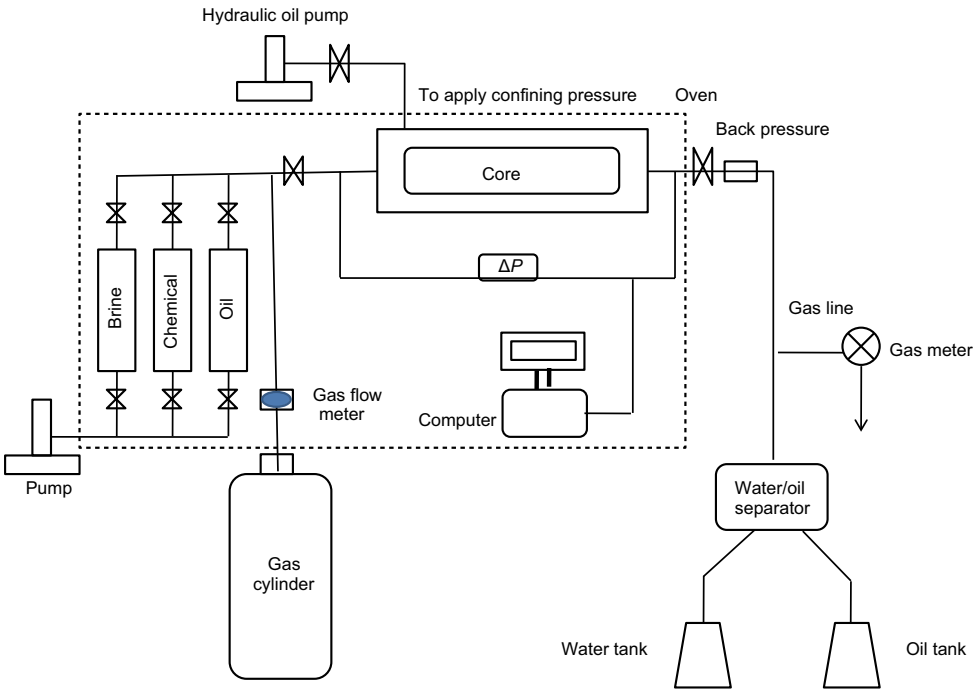

Fig. 1 Schematic diagram of a setup for coreflood displacements

mechanisms involved in the CWAG process. A set of PVT experimental results are also presented to elucidate the effects of CO_2 interactions with oil in terms of viscosity reduction and oil swelling.

3 Chemical screening and formulation

To achieve the main objective of this study, it is desirable to design an ASP slug which can produce a low IFT system and provide good mobility control during coreflood tests. The details of the chemical screening and formulation are presented in the following sub-sections.

3.1 Surfactant screening

The selected crude oil was tested using three suitable available surfactants in a surfactant screening test. The purpose of the surfactant screening test was to find a surfactant and concentration that would generate a high solubilization ratio at optimum salinity which corresponds to the attainment of an ultralow IFT. The selected surfactant could then be used for further studies and optimization with other chemical additives. The phase behavior study of the surfactant screening is presented in Table 1. It shows that Test A-3 produced the highest solubilization ratio as compared to the other types of surfactants. The surfactant used in Test A-3 is Petrostep S13C which is alcohol alkoxy sulfonate. A solubilization ratio of nine at an optimum salinity of 1.6 wt% was obtained from this surfactant. This surfactant was selected for further experimentation.

3.2 Effect of surfactant concentration

To examine the performance of surfactant in terms of high solubilization ratio and IFT reduction at different concentrations and to understand the dilution effect of surfactant in reservoir applications, a series of phase behavior experiments were conducted with Petrostep S13C with relatively high to low concentrations. The results are tabulated in Table 2. The results show that the optimal solubilization ratio decreases slightly from 12 to 9 and to 8 mL/mL as the concentration is reduced from 2 to 1 and 0.5 wt%, respectively. Thus, as the total surfactant concentration decreases, the optimal solubilization ratio also decreases. This means that the surfactant performance decreases at lower surfactant concentrations. The results also show that the optimal salinity increases slightly from 1.35 to 1.9 wt% NaCl as the surfactant concentration is decreased from 2 to 0.5 wt% (Table 2). In summary, the results of Table 2 show that the optimal solubilization ratio remains nearly constant at low surfactant concentrations of 0.5 wt% (with optimum solubilization ratio of eight) and 1 wt% (with optimum solubilization ratio of nine). There are some cost advantages with injecting dilute surfactants even for a fixed mass of surfactant. The surfactant concentration of 0.5 wt% was selected for final chemical formulation involving Petrostep S13C.

3.3 Alkaline selection and optimization

A series of experiments with an aqueous solution containing 0.5 wt% surfactant, and different concentrations of sodium carbonate as alkali were conducted with the selected crude oil. Salinities ranging from 0 to 3 wt% NaCl were prepared to observe all microemulsion types for different concentrations of alkali. The data from phase behavior tests are presented in Table 3. The results show that an increase in the alkali concentration causes an increase in the optimal solubilization ratio up to 11, which is a result of the in situ generated surfactant (soap) due to the reaction between the alkali and the acidic components of oil. There is a slight decrease in optimum salinity with increased alkali concentration, which is likely due to the generation of in situ surfactant. The in situ surfactant may have an optimal salinity lesser than that of the synthetic surfactant, and therefore its presence would decrease the optimal salinity. The 0.5 wt% alkali concentration (with

Table 2 Microemulsion phase behavior tests conducted for surfactant concentration selection

Tests	Petrostep S13C, wt%	NaCl scan, wt%	Optimal salinity, wt% NaCl	Optimal solubilization ratio, mL/mL
B-1	2	0–4	1.35	12
A-3	1	0–4	1.6	9
B-2	0.5	0–4	1.9	8

Table 1 Microemulsion phase behavior tests conducted for surfactant screening

Tests	Surfactant	Surfactant concentration, wt%	NaCl scan, wt%	Optimal salinity, wt% NaCl	Optimal solubilization ratio, mL/mL
A-1	Petrostep S13A	1	0–4	2.3	4.5
A-2	Petrostep S3B	1	0–2	1.3	5
A-3	Petrostep S13C	1	0–4	1.6	9

0.5 wt% surfactant concentration) was selected as the economic concentration which provided a high optimal solubilization ratio of ten.

3.4 ASP slug formulation

As discussed in the last three sub-sections, the microemulsion phase behavior study for the selected crude oil shows a good performance in achieving a high solubilization ratio over a range of surfactant and alkali concentrations. This information was used to design a chemical recipe suitable for the intended coreflood experiment.

A total surfactant concentration of 0.5 wt% was chosen based on the data in Table 2. The 0.5 wt% surfactant concentration results in a solubilization ratio as high as 8, which is sufficient to produce a low IFT system. The results obtained when considering alkali in phase behavior experiments with a fixed 0.5 wt% surfactant concentration are given in Table 3. The experimental data show that the highest solubilization ratios of 11 and 10 occur for 1 and 0.5 wt% Na_2CO_3, respectively. Since there is not much difference in solubilization ratio when the alkaline concentration is doubled, the 0.5 wt% alkaline was used in chemical formulation with an optimum salinity of 1.2 wt% higher than the salinity of injection brine (1 wt%). Thus, the chemical recipe C-1 with 0.5 wt% surfactant and 0.5 wt% alkali concentrations with an optimum salinity of 1.2 wt% was selected for further tests. A concentration of 0.15 wt% SNF-3330S polymer was incorporated in the chemical slug for the mobility control during coreflood. Polymers affect the relative mobility of the phases generated during a chemical flood, but they do not appear to affect the solubilization of phases, so the system follows the typical pattern of a microemulsion system without polymer. Polymer viscosity versus concentration data at a temperature of 85 °C and a salinity of 1.2 wt% (salinity of the chemical slug) is shown in Fig. 2. This figure gives an approximate estimate of the slug viscosity in coreflood experiments. The ASP slug formulation is presented in Table 4.

Table 3 Microemulsion phase behavior tests conducted for alkali selection and optimization

Tests	Petrostep S13C, wt%	Na_2CO_3, wt%	NaCl scan, wt%	Optimal salinity, wt% NaCl	Optimal solubilization ratio, mL/mL
B-2	0.5	0	0–3	1.9	8
C-1	0.5	0.5	0–3	1.2	10
C-2	0.5	1	0–3	0.6	11

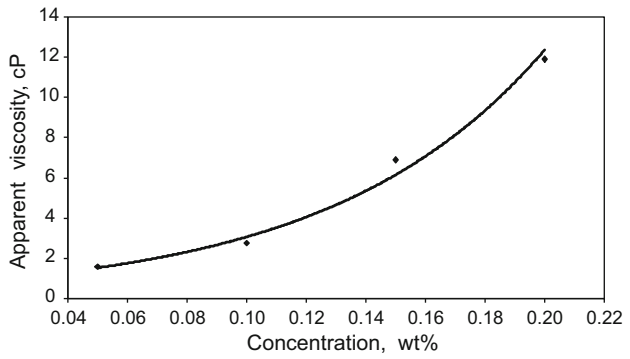

Fig. 2 Polymer viscosity versus concentration at 1.2 wt% NaCl and 85 °C

4 Coreflood experiments

WAG and CWAG coreflood experiments were performed on a Berea sandstone core. WAG coreflood provided a basis for comparing the results of CWAG as a new EOR method. The chemical recipe provided in Table 4 was used in the CWAG coreflood experiment. A low concentration of polymer was used in the CWAG coreflood to avoid plugging and also provided enough viscosity to create a favorable mobility ratio in the coreflood. The injection rate was set to 2 ft/D, roughly twice that for waterflooding (typically at approximately 1 ft/D), and was constant during the coreflood experiment. Table 5 lists the measured and calculated core property data on the Berea sandstone core obtained during core preparation and initial flood experiments.

Table 5 Measured and calculated properties of Berea core

Parameters	Value
Mass (dry core) m, g	670
Length L, cm	30.48
Diameter D, cm	3.81
Pore volume, mL	76.45
Porosity φ	0.22
Permeability to air (bare core) k_{air}, mD	214
Permeability to brine k_{br}, mD	192.13
Connate water saturation S_{wc}	0.21
Initial oil saturation S_{oi}	0.79

Table 4 Optimum chemical formula used during CWAG coreflood experiments

Tests	Petrostep S13C, wt%	Na_2CO_3, wt%	SNF-3330S, wt%	NaCl salinity, wt%
D-1	0.5	0.5	0.15	1.2

Table 6 Injection and recovery data of WAG and CWAG coreflood experiments

Parameters	Coreflood data	WAG	CWAG
Injection data	Flow rate, mL/h and ft/D	0.2, 1	0.2, 1
	ASP slug size, PV	–	0.6
	CO_2 slug size (in each cycle), PV	0.6	0.6
	Water slug size, PV	0.6	0.6
Recovery data	Waterflood, % OOIP	64	64
	EOR, % ROIP and % OOIP	22, 8	48.6, 17.5
	Total, % OOIP	72	81.5

Notes: ROIP is the abbreviation for remaining oil in place after waterflooding

During the WAG coreflood, three cycles of WAG were injected into the core. Each cycle included 0.6 PV of CO_2 and 0.6 PV of water. CWAG coreflood followed the WAG process, without interrupting the coreflood experiment. Therefore, the CWAG began after three cycles of initial WAG. This procedure helped understand the potential of CWAG in improving oil recovery compared to that of only WAG injection. Also it helped in observing the effect of an ASP slug on the recovery when there was no more oil production from the WAG process. During CWAG, the initial WAG was followed by a 0.6 PV ASP slug and displaced by two more cycles of WAG. The coreflood results are shown in Table 6. It is seen that CWAG improved the WAG oil recovery by 26.6 %. This result demonstrates the potential of CWAG as a new EOR method by improving the oil recovery significantly. The following sections discuss the results according to oil recovery and differential pressure response during coreflood experiment.

4.1 Oil recovery

Figure 3 shows the cumulative remaining oil recovery after waterflooding (ROIP) as a function of the injection pore volume (PV) during WAG injection. During the first CO_2 slug injection, 8.4 % ROIP was recovered. This is apparently related to the invasion of CO_2 into those pores which are inaccessible by water (Dong et al. 2005). After 0.6 PV of CO_2 slug injection, 0.6 PV of water was injected into the core, resulting in additional 6.2 % ROIP oil recovery. Figure 3 shows that 14.6 and 6.3 % of ROIP were recovered during the first and second WAG cycles, respectively, compared to 0.1 % ROIP recovery during the third cycle. It means that the major portion of the oil is obtained from the first and second cycles of WAG injection. Because of the increasingly high water saturation and reduced discontinuity of the oil phase, the oil recovery declined significantly after second cycle. The oil recovery by WAG injection was 22 % ROIP for a total oil recovery (including waterflooding) of 72 % OOIP.

Figure 4 shows the residual oil recovery during the CWAG process as a function of the fluid pore volume

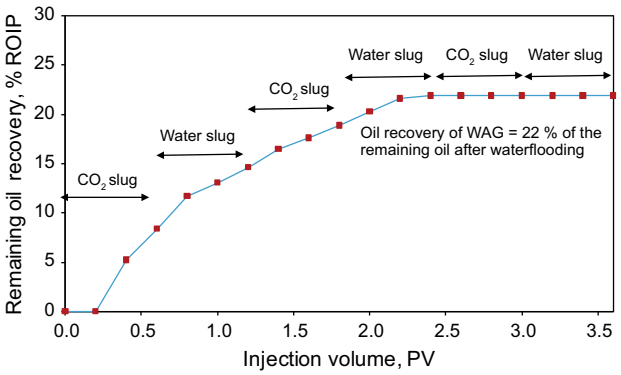

Fig. 3 Cumulative remaining oil recovery after waterflooding for WAG coreflood experiments. Three cycles of WAG, including 0.6 PV of CO_2 and 0.6 PV of water in each cycle were injected

injected. As aforementioned, the initial 3 cycles of WAG could only recover 22 % ROIP. The CWAG process then started by injecting a 0.6 PV ASP slug that was followed by two cycles of WAG. Figure 4 shows that during ASP slug injection, there is no oil production until the oil bank breaks through from the core because the oil is initially at residual saturation in a tertiary flood. In CWAG coreflood, the final oil recovery was 48.6 % ROIP which is more than twice that of the WAG process—a 26.6 % improvement over the WAG process. The total oil recovery from the CWAG process including the waterflooding stage was 81.5 % OOIP.

Figure 5 shows that there are two noticeable oil banks after ASP slug injection. The first oil bank is related to the ASP slug itself. The ASP slug was injected at an optimal salinity which would produce microemulsion Type III immediately after contact with residual oil. The microemulsion Type III has an ultralow IFT, and it can mobilize the residual oil left after the 3 cycles of initial WAG injection. The higher viscosity of the ASP (refer to Fig. 2) compared to that of water improves the sweep efficiency and makes new flow channels in unswept regions of the core pushing out more bypassed oil. The second oil bank could be related to surfactant desorption. Since the

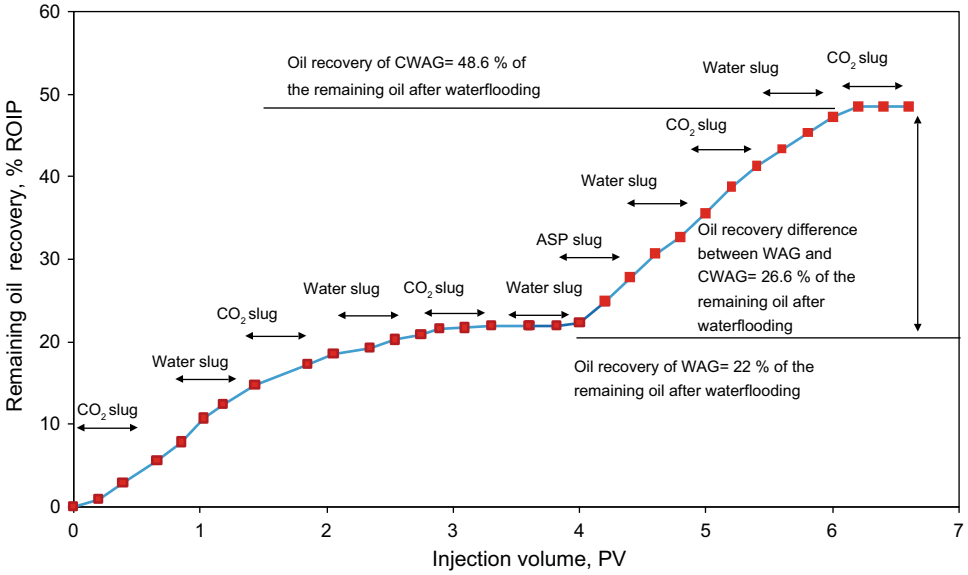

Fig. 4 Cumulative remaining oil recovery after waterflooding for the CWAG coreflood experiment. In the CWAG process, an ASP slug was injected after three initial WAG cycles and followed by two more WAG cycles. Each WAG cycle included 0.6 PV of CO_2 and 0.6 PV of water, WAG ratio was 1; ASP slug size was 0.6 PV

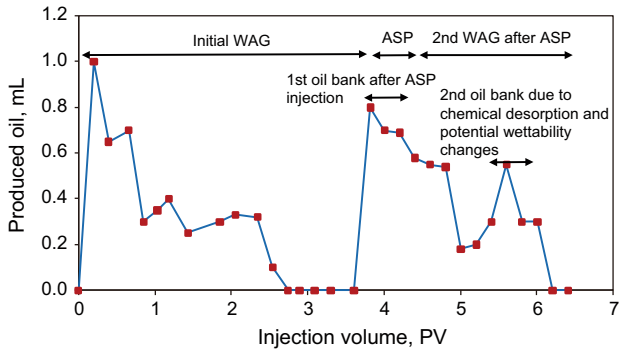

Fig. 5 Oil produced during the CWAG process. There are two noticeable oil banks after injection of the ASP slug which was injected after the initial WAG when there was no more oil production

first water slug after ASP has a lower salinity than ASP, a negative salinity gradient was imposed in the coreflood. A negative salinity gradient allows the generation of microemulsion Type I and, thus trapped surfactant is mobilized into the water slug again through surfactant desorption. It is also possible that alternate injection of water and CO_2 after ASP slug may have changed the wettability of the rock surfaces to make them more water wet. Due to the presence of the trapped CO_2, the natural tendency of the water drive (after ASP) to move unhindered in the water-wet channels is significantly reduced. Trapped CO_2 also helps reduce the overriding of the water drive in the ASP slug and generate microemulsion in the preferentially oil-filled channels which contain the residual oil.

4.2 Differential pressure response

Figure 6 shows the differential pressure curve during three cycles of WAG followed by an ASP slug and two more WAG cycles. After waterflooding, EOR was commenced by CO_2 slug injection in WAG mode. At the beginning of the first CO_2 slug, the differential pressure was low because of low viscosity of CO_2. But shortly after mobilizing the residual oil by CO_2, the differential pressure increased to its maximum value of 3.1 psi and then decreased slowly as the injection continued and the mobilized oil was produced.

During the first water slug injection following the CO_2 slug, a sudden increase in differential pressure was observed that was related to a sudden change in the viscosity of the injected fluid from CO_2 to water and also mobilizing a new batch of oil in the core. The first slug of CO_2 injection changed the mobility of the water in the core, and thus the water slug following the CO_2 slug recovered some more oil. Also some oil which was moved to the water channels during previous CO_2 injection was produced during this step. Figure 6 shows that the second and third cycles of WAG behaved in the same way as was previously explained.

After three cycles of WAG, when there was no more oil production, an ASP slug was injected into the core and then displaced by alternate injection of water and CO_2. There was an increase in differential pressure during the ASP slug injection which shows a flow resistance related to the formation and propagation of the oil bank in the core due to

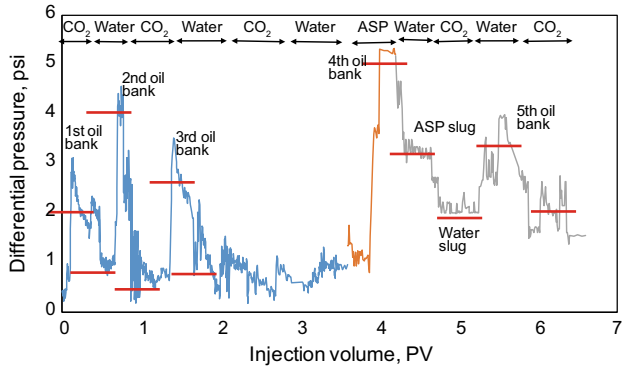

Fig. 6 Differential pressure response during the first three cycles of WAG, the ASP slug, and the second two cycles of drive WAG. Each WAG cycle included 0.6 PV of CO_2 and 0.6 PV of water, WAG ratio was 1; ASP slug size was 0.6 PV

ASP injection. The increase in differential pressure is due to the mobilization of residual oil which persisted until oil bank breakthrough. The mobilized oil creates an oil bank in front of the ASP slug. As the oil bank size increases, the differential pressure increases until oil bank breakthrough occurs. The second peak in the differential pressure is related to the second oil bank generated that is associated with surfactant desorption and wettability changes. After the second oil bank breakthrough and microemulsion production, the conditions in the core and the differential pressure profile are similar to that in the previous WAG process but slightly higher. This is possibly due to chemical slug effects such as adsorption and wettability changes.

5 Important parameters affecting CWAG process

To improve the CWAG performance, it is desirable to identify the key parameters that have the most significant effect on the CWAG process. In any EOR method, the aim is to maximize the microscopic and macroscopic sweep efficiencies. The volumetric sweep efficiency is improved by maintaining a favorable mobility ratio between the displacing and displaced fluids. The microscopic displacement efficiency of the CWAG process depends greatly on the phase behavior of the CO_2, water, and reservoir oil mixture. CO_2 can dissolve easily into oil, reduce oil viscosity, swell the oil and it can extract the light components of oil. IFT reduction is another important parameter that affects the CWAG process. The effects of mobility control, IFT reduction, and interactions of CO_2 with oil on the CWAG process are further discussed in the following sub-sections.

5.1 Mobility control

The CWAG process claims an improvement of the WAG mobility ratio, M. It affects both the areal and vertical sweeps, with sweep increasing as M decreases for a given volume of fluid injected. In a CWAG process, there is more than one displacement front due to the injection of multiple slugs of different fluids such as ASP, CO_2, and water. The flow behavior of any specific displacement front is affected by the mobilities of the fluids immediately ahead of and behind that front and also by the mobilities of the fluids in the regions around the other fronts.

The mobility ratio between the displaced and displacing phases is calculated from the differential pressure data obtained from coreflood experiments. The average sectional differential pressure is determined through the differential pressure curve shown in Fig. 6. The mobility ratio was calculated for different slug injections during the WAG and CWAG processes. For the WAG injection, the average value of the differential pressure during the flow of displacing phases is determined, and the mobility ratio between the oil bank and displacing phases is calculated for different cycles of WAG injection as follows (by combining mobility ratio and Darcy's law):

1st oil bank and drive: $M = [\Delta p_{(1\text{st oil bank})}/\Delta p_{(\text{drive})}] = 2.2/1 = 2.2$,

2nd oil bank and drive: $M = [\Delta p_{(2\text{nd oil bank})}/\Delta p_{(\text{drive})}] = 3.4/0.8 = 4.2$,

3rd oil bank and drive: $M = [\Delta p_{(3\text{rd oil bank})}/\Delta p_{(\text{drive})}] = 2.6/1 = 2.6$,

After three cycles of WAG injection when there was no more oil production, an ASP slug was injected into the core and it is driven by two more WAG cycles which is named as CWAG. During CWAG, the mobility is calculated as follows:

4th oil bank and drive: $M = [\Delta p_{(4\text{th oil bank})}/\Delta p_{(\text{drive})}] = 4.6/3.2 = 1.4$

5th oil bank and drive: $M = [\Delta p_{(5\text{th oil bank})}/\Delta p_{(\text{drive})}] = 3.5/2.1 = 1.6$

It can be seen from the above simple calculations that in the CWAG process there is a better mobility control (the lower the mobility ratio, the higher the mobility control) during CWAG compared to WAG flooding. Also good mobility control is achieved between the ASP slug and the polymer-free water drive which was pushing the ASP slug. The mobility ratio is calculated as follows:

Mobility ratio: $M = [\Delta p_{(\text{ASP})}/\Delta p_{(\text{polymer-free water drive})}] = 3.2/2.1 = 1.5$.

It is very important that CWAG permits the use of a polymer-free water drive to push the ASP slug. This is due to the trapped CO_2 in the core which directs ASP and water drive to move in oil-filled channels which contain the residual oil and microemulsion.

5.2 IFT reduction

To minimize the water blocking effect during WAG process, it is proposed to have an ultralow IFT system using

alkali and surfactant. The solubilization result for the phase behavior of Test C-1 is presented in Fig. 7. This result can be used to predict the IFT of the alkali–surfactant system against crude oil using Huh's correlation. The IFT computed from Huh's equation is plotted in Fig. 8 as a function of salinity. In optimum salinity (1.2 wt%), the IFT between oil/microemulsion and water/microemulsion is equal and that is the occasion when the IFT is the lowest. During ASP slug injection, the injected surfactant mixes with the surfactant generated in situ by the chemical reactions between the alkaline and the natural organic acids in the crude oil which result in an ultralow IFT. The amount of surfactant generated in situ depends on the acid value of the crude oil. The ultralow IFT at the oil–brine interface helps emulsify and mobilize the residual oil in the reservoir. The produced microemulsion during coreflood experiment confirms that there is a reduction in IFT during ASP slug injection which causes aqueous and oil phase partitioning.

5.3 Effects of CO_2 interactions with oil

To demonstrate the effects of CO_2 on oil viscosity reduction and swelling, a set of PVT experiments were performed with dead oil (oil with no dissolved gases). To study the effect of CO_2 on oil, approximately 50 mL of the oil was transferred into a preheated PVT cell, and then CO_2 was added to the oil in a series of steps from 20 to 80 mol percent of the oil. At each addition, homogeneity of the mixture was achieved by magnetically stirring the mixture until the PVT cell pressure was stabilized at the set value. Constant composition expansion (CCE) tests were conducted after adding a predetermined amount (in mole percent) of CO_2. A sample of CO_2-added oil was transferred to an electromagnetic viscometer to measure the viscosity. The CO_2-saturated oil properties are presented in Table 7.

The saturation pressures of all the CO_2-saturated oil mixtures were determined by the break in the pressure–volume curves attained from CCE tests. The viscosities of all the mixtures were measured at pressures slightly above their bubble point pressures using a viscometer, and by a short linear extrapolation it was possible to determine the related values at saturation pressure. The oil swelling factor is calculated as the ratio of CO_2-saturated oil volume at the saturation pressure to the oil volume at the bubble point pressure (p_b) at 85 °C.

The saturation pressures versus CO_2 added data obtained from the experiments are plotted in Fig. 9. As expected, the saturation pressure increases with CO_2 addition. This implies that the solubility of CO_2 is a function of pressure.

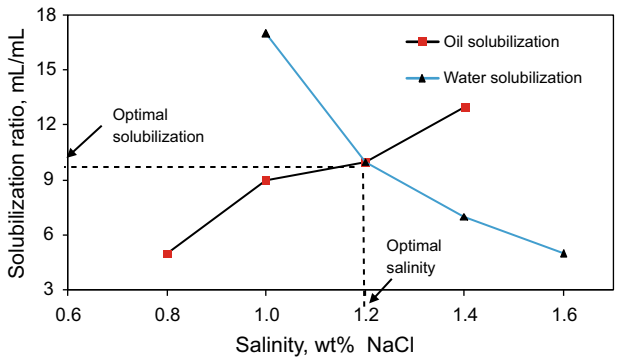

Fig. 7 Solubilization ratio versus salinity for phase behavior of Test C-1

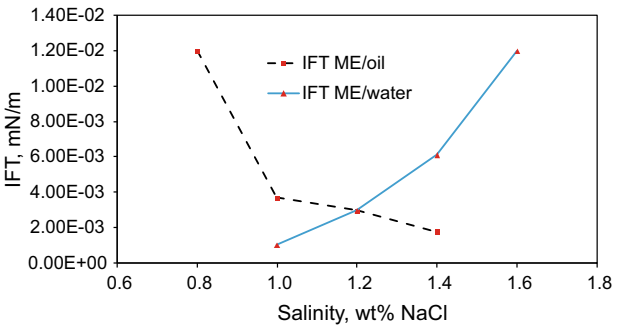

Fig. 8 IFT calculated from Huh's equation for Test C-1 (ME is the abbreviation for microemulsion)

Table 7 CO_2-saturated dead oil properties

Fluid	CO_2 added, mol%	Saturation pressure, psi	Mixture viscosity at p_{sat}, cP	Swelling factor
Dead oil	0	14.5	1.6	1
CO_2-saturated oil	20	350	1.35	1.05
	40	778	1.08	1.15
	60	1540	0.7	1.33
	80	3066	0.4	2.12

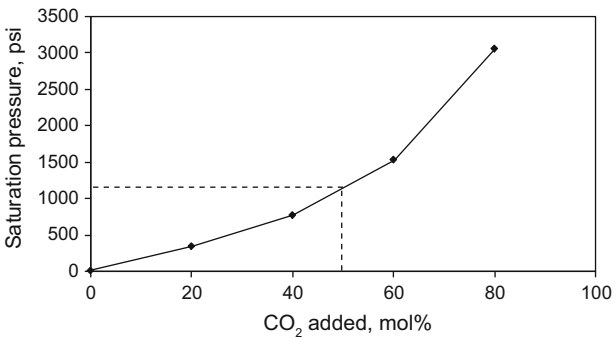

Fig. 9 Saturation pressure versus volume of added CO_2 in dead oil. With a back pressure of 1200 psi during CWAG coreflood, a 50 mol% CO_2 solubility is expected

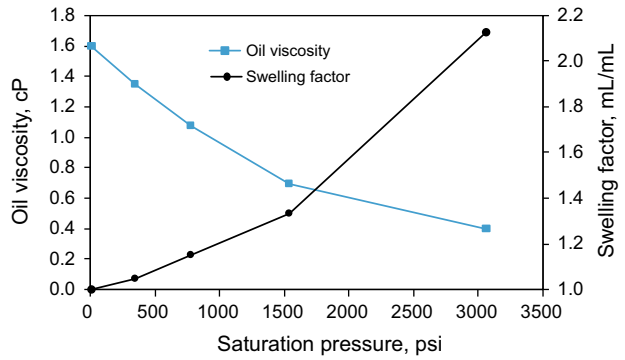

Fig. 10 Viscosity and swelling factor curves of CO_2-saturated oil at 85 °C; with back pressure of 1200 psi during CWAG coreflood; a swelling factor of 1.25 (an increase in oil volume by 25 %) and a reduction in oil viscosity from 1.6 to 0.83 cP are expected

The more CO_2 is dissolved, the higher is the saturation pressure. The dissolution of CO_2 into the oil is also a function of temperature and oil composition. The saturation pressure increases steadily as the mole fraction of CO_2 increases, and reached 3066 psi at 80 mol%. It is also concluded from Fig. 9 that with a back pressure of 1200 psi during CWAG coreflood, a minimum of 50 mol% CO_2 solubility is expected during the CWAG process.

Figure 10 shows the related results for swelling factor and viscosity curves of CO_2-saturated oil at 85 °C. In a CO_2 injection process, the dissolution of CO_2 into the oil can result in varying degrees of oil swelling, depending on the oil properties. An increase in oil volume will allow discontinuous oil droplets trapped in a porous medium to merge with the flowing oil phase. The swelling factor (SF) curve rises smoothly as the saturation pressure increases (Fig. 10). The experimental results indicate that approximately 100 % expansion of the reservoir fluid can be expected at a pressure of 3066 psi.

Figure 10 also shows that CO_2 could significantly reduce the viscosity of oil at a relatively low pressure. Experimental results showed that the CO_2-saturated oil viscosity decreased sharply as more CO_2 was absorbed with the increasing saturation pressure. The viscosity of the oil ranged from 1.6 cP in dead oil to 0.4 cP for 80 mol% of CO_2 dissolved in the oil. By considering a back pressure of 1200 psi during CWAG coreflood experiments, the oil swelling factor was 1.25, indicating that the oil volume increased by 25 %. The oil viscosity was reduced to 0.83 cP at 1200 psi from its original viscosity of 1.6 cP.

6 CWAG simulation approach

The CMG–STARS simulator was used to numerically model and simulate the CWAG process. CMG–STARS is a finite-difference, thermal, *K* value compositional, chemical reaction and geomechanics reservoir simulator ideally suited for advanced modeling of recovery processes (CMG 2011). In this study, the effects of oil swelling and oil viscosity reduction which are the two important mechanisms in immiscible CO_2 flooding are modeled via appropriately chosen pressure–temperature-dependent *K* values describing solubility, as well as compositionally dependent viscosities. CMG–STARS can handle a reduction in IFT of a maximum of two components. Surfactant and alkali components are responsible for IFT reduction in the simulation model. The reduction of IFT is usually correlated with decreased residual oil (and connate water) and change in relative permeability through the calculation of a dimensionless capillary number describing the balance between viscous and interfacial forces. STARS can interpolate between different sets of relative permeability curves based on capillary number. In addition, the presence of surfactants can alter rock wettability, usually interpreted as a change in the curvature of water and oil relative permeability curves. The water rheological properties which are a function of polymer concentration are handled with the polymer option in STARS.

6.1 History matching of coreflood experimental data

A Cartesian rectangular coordinate grid was used to describe the coreflood experiment. 100 grid blocks in the flow direction were specified to increase the simulation accuracy and to improve the convergence. The number of grid blocks in the other directions was set equal to unity to simulate 1-D flow. The porosity and permeability values were assumed to be unchanged by mineral dissolution or precipitation reactions. The details of reservoir rock and fluid properties as well as grid block sizes used in simulation are presented in Table 8.

Six components (water, oil, CO_2, alkali, surfactant, and polymer) were modeled to simulate the CWAG processes. Three phases present in the simulation are aqueous, oleic, and gaseous phases. The oil component can partition into the aqueous phase in the presence of surfactant. The partitioning of oil in the aqueous phase results in a low IFT between the aqueous phase and the oil phase. The IFT data are used to calculate a set of capillary numbers in the simulation model. The change in the capillary number translates into a change in relative permeability and a reduction in the residual oil saturation. During history matching, relative permeability is a variable parameter adjusted to match the coreflood data. The gas–oil relative permeability curves were also generated by Corey (1954) correlations in each case. It is also important to mention that due to the effect of CO_2, the liquid/CO_2 relative permeability curves may change with CO_2 concentration when CO_2 injection causes oil and CO_2 phases to mix. The

Table 8 Reservoir and fluid properties on coreflood simulation

Reservoir properties		Fluid properties	
Parameters	Values	Parameters	Values
Grid size, cm	[0.1, 98 × 0.30897, 0.1] × 3.38 × 3.38	Water density, g/cm^3	0.976
Grid	100 × 1×1	Water viscosity, cP	0.44
$k_x \times k_y \times k_z$, mD	192.13 × 192.13 × 192.13	Oil density, g/cm^3	0.835
Porosity	0.21	Oil viscosity, cP	1.6
Reservoir pressure, psi	1200	Initial oil saturation	0.79
Reservoir temperature, °C	85	Connate water saturation	0.21
Rock type	Sandstone		

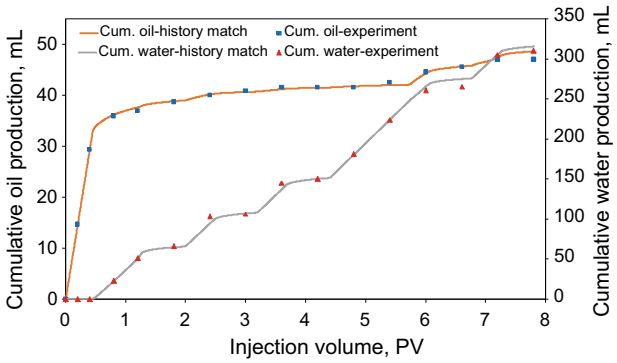

Fig. 11 History matching of cumulative oil production and water production during WAG injection of the CWAG process

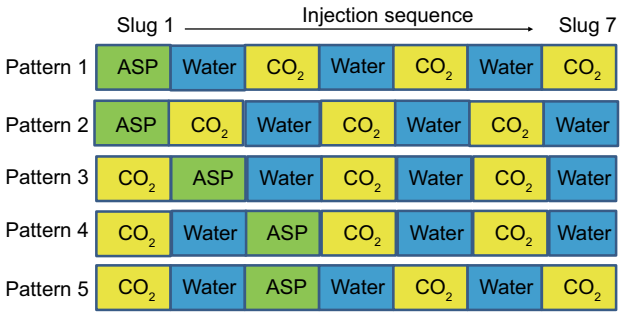

Fig. 12 Different slug patterns of the CWAG process

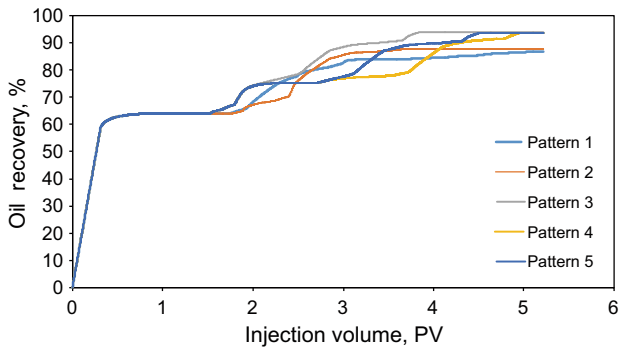

Fig. 13 Oil recovery factor for different CWAG slug patterns

correct values of CO_2/liquid relative permeability were achieved during history matching. The Stone model II (modified) method was used to utilize the two-phase relative permeability measurements as a correlation of the three-phase relative permeability curves (Aziz and Settari 1979). The adsorption capacity of rock to polymer, alkali, and surfactant was also considered during history matching. Figure 11 shows the experimental oil recovery and cumulative water production overlain by simulated data for the CWAG coreflood experiment. Figure 11 shows a satisfactory match for the coreflood data. Only minor experimental irregularities in cumulative water production, such as 2.4, 3.6, and 6.6 PV were not matched.

6.2 Sensitivity analysis

The history-matched model was used for a sensitivity study. A sensitivity analysis is performed on the critical parameters affecting the process significantly, such as slug pattern and CO_2 slug size.

To study the effect of the CWAG slug pattern, five different patterns as presented in Fig. 12 were considered with the same chemical composition used in the coreflood experiment. All slug patterns are designed with an initial 1.2 PV waterflooding. This study helps identify which pattern yields a better recovery during the CWAG process. The effects of slug pattern on CWAG performance are presented in Figs. 13, 14 and 15. Figure 13 shows that Patterns 3, 4, and 5 give almost the same recovery which is higher than that of both Patterns 1 and 2.

The simulation results confirmed that if the ASP slug is injected after the initial CO_2, it would be more beneficial compared to the injection of the ASP slug before CO_2. In this study, it is found that slug Pattern 3 has the best performance during the whole injection period compared to other patterns. This shows that injection of an ASP slug which is preceded by only one cycle of CO_2 slug and followed by alternating water and CO_2 injection provides a better practical pattern for the CWAG process. This is due

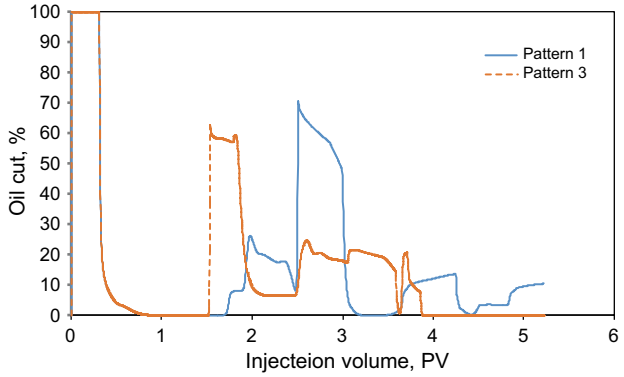

Fig. 14 Oil cut for the slug Patterns 1 and 3 of the CWAG process

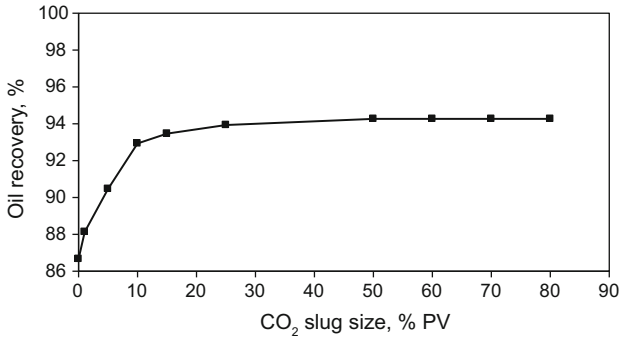

Fig. 16 The effect of initial CO_2 slug size in the CWAG process

to the oil viscosity reduction which resulted from the injection of initial CO_2 in front of the ASP slug. The reduction in oil viscosity consequently improves the areal sweep efficiency of ASP flooding as well as its injectivity.

Figure 14 shows oil cuts for Patterns 1 and 3 which have the lowest and highest ultimate oil recovery in CWAG patterns, respectively. It shows that in Pattern 3, there is an oil bank formed after the CO_2 and ASP slugs which produces continuously over a period of time. It means that there is a good mobility control in Pattern 3. In contrary, the oil cut during Pattern 1 decreases sharply during the ASP slug oil bank production which means an unfavorable mobility ratio is found that results in less oil recovery in Pattern 1.

Figure 15 shows the average pressure during the slug Patterns 1 and 3. During the initial CO_2 injection, in Pattern 3, there is a decreasing trend in the average reservoir pressure due to low viscosity of CO_2. It is then followed by ASP and water slugs which cause an increase in average pressure. During CO_2 and water slug injection after the ASP slug, the differential pressure decreases and increases alternately. A higher differential pressure during Pattern 3 compared to that of Pattern 1 is due to displacement of the larger oil bank in Pattern 3. This result shows that injection of CO_2 slug before the ASP slug is beneficial during a CWAG process.

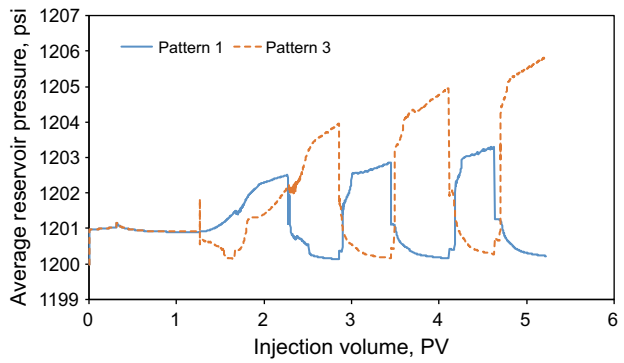

Fig. 15 Differential pressure for slug Patterns 1 and 3 of the CWAG process

A series of sensitivity tests was conducted to investigate the effect of initial CO_2 slug size during the CWAG process. It is shown that having an ASP slug after the initial CO_2 slug is crucial in recovering more oil from the reservoir. Figure 16 shows the oil recovery versus initial CO_2 slug size. This demonstrates that using 25 % PV CO_2 slug at the front of ASP, the CWAG oil recovery can be maximized. This result suggests that there is an optimum size for the CO_2 slug at the front of the ASP slug. Injecting more than the optimum CO_2 slug size is not recommended to prevent asphaltene deposition. The initial CO_2 slug reduces the residual oil saturation and oil viscosity, and causes oil swelling.

7 Conclusions

In this work, a new EOR method, CWAG, is proposed to improve the oil recovery from the conventional WAG process by combining two commercially competitor processes, i.e., ASP and WAG. The most important conclusions that can be drawn from this study are as follows:

(1) The CWAG method achieves 26.6 % more than twice the incremental recovery of WAG.
(2) The CWAG process significantly reduces the IFT and provides an ultralow IFT system to minimize the water blocking effect.
(3) As well, CWAG has more favorable mobility compared to WAG.
(4) The injection sequence is important in the CWAG process. Injection of an ASP slug after one slug of CO_2 results in higher incremental oil recovery.
(5) In the CWAG process, there is an optimum CO_2 slug size for maximum possible recovery (25 % PV is sufficient).

Acknowledgments The authors would like to thank the EOR Center at University Technology Petronas for providing financial support, materials, and experimental equipment for this work. We also thank laboratory assistants Mr. Riduan B. Ahmad and Mr. Saiful N. Ismail for their help with laboratory experiments and data analysis. We also would like to acknowledge Mr. Ahmad Y. Talib from MECAS, UZMA Bhd. and Stepan Company for providing surfactant samples.

References

Al-Abri A, Amin R. Phase behaviour, fluid properties and recovery efficiency of immiscible and miscible condensate displacements by $SCCO_2$ injection: experimental investigation. Transp Porous Med. 2010;85(3):743–56. doi:10.1007/s11242-010-9589-5.

Aziz K, Settari A. Petroleum reservoir simulation. London: Applied Science Publishers Ltd; 1979.

Caudle BH, Dyes AB. Improving miscible displacement by gas-water injection. In: The 32nd annual fall meeting of Society of Petroleum Engineers, Dallas, Texas; 1958. doi:10.2118/911-G.

Christensen JR, Stenby EH, Skauge A. Review of WAG field experience. SPE Reserv Eval Eng. 2001;4(2):97–106. doi:10.2118/71203-PA.

CMG: STARS user's guide. Version 2011. 10, Calgary, Canada; 2011.

Corey AT. The interrelation between gas and oil relative permeabilities. In: The 18th technical conference on petroleum production, Pennsylvania; 1954.

Dehghan AA, Farzaneh SA, Kharrat R, et al. Pore-level investigation of heavy oil recovery during water alternating solvent injection process. Transp Porous Med. 2010;83(3):653–66. doi:10.1007/s11242-009-9463-5.

Dong M, Foraie J, Huang S, Chatzis I. Analysis of immiscible water-alternating-gas (WAG) injection using micromodel tests. J Can Pet Technol. 2005;44(2):17–25. doi:10.2118/05-02-01.

Faisal A, Bisdom K, Zhumabek B, et al. Injectivity and gravity segregation in WAG and SWAG enhanced oil recovery. In: SPE annual technical conference and exhibition, New Orleans, Louisiana; 2009. doi:10.2118/124197-MS.

Flaaten A, Nguyen QP, Pope GA, Zhang J. A systematic laboratory approach to low-cost, high-performance chemical flooding. SPE Reserv Eval Eng. 2009;5:713–23. doi:10.2118/113469-PA.

Green DW, Willhite GP. Enhanced oil recovery. Richardson: SPE; 1998.

Hinderaker L, Utseth RH, Hustad OS, et al. RUTH—a comprehensive Norwegian R & D program on IOR. In: European petroleum conference, Milan, Italy; 1996. doi:10.2118/36844-MS.

Huh C. Interfacial tensions and solubilizing ability of a microemulsion phase that coexists with oil and brine. J Colloid Interface Sci. 1979;71(2):408–26. doi:10.1016/0021-9797(79)90249-2.

Kulkarni MM. Immiscible and miscible gas-oil displacements in porous media. MS thesis. Louisiana State University. 2003.

Levitt D, Dufour S, Pope GA, et al. Design of an ASP flood in a high-temperature, high-salinity, low-permeability carbonate. In: The international petroleum technology conference, Bangkok, Thailand; 2011. doi:10.2523/14915-MS.

Lin EC, Huang ETS. The effect of rock wettability on water blocking during miscible displacement. SPE Reserv Eng. 1990;5(2):205–12. doi:10.2118/17375-PA.

Liu S, Miller CA, Li RF, Hirasaki G. Alkaline/surfactant/polymer processes: wide range of conditions for good recovery. SPE J. 2010;15(2):282–93. doi:10.2118/113936-PA.

Martin FD, Kovarik FS, Chang P, et al. Gels for CO_2 profile modification. In: SPE enhanced oil recovery symposium, Tulsa, Oklahoma, USA; 1988. doi:10.2118/17330-MS.

Muller T, Lake LW. Theoretical study of water blocking in miscible flooding. SPE Reserv Eng. 1991;6(4):445–51. doi:10.2118/20206-PA.

Rao DN, Ayirala SC, Kulkarni MM, et al. Development of gas assisted gravity drainage (GAGD) process for improved light oil recovery. In: SPE/DOE symposium on improved oil recovery, Tulsa, Oklahoma, USA; 2004. doi:10.2118/89357-MS.

Ruckenstein E. Evaluation of the interfacial tension between a microemulsion and the excess dispersed phase. Soc Petrol Eng J. 1981;21(5):593–602. doi:10.2118/9281-PA.

Sharma A, Rao DN. Scaled physical model experiments to characterize the gas-assisted gravity drainage EOR Process. In: SPE/DOE symposium on improved oil recovery, Tulsa, Oklahoma, USA; 2008. doi:10.2118/113424-MS.

Tchelepi HA, Orr FM. Interaction of viscous fingering, permeability heterogeneity, and gravity segregation in three dimensions. SPE Reserv Eng. 1994;9(4):266–71. doi:10.2118/25235-PA.

Walker D, Britton C, Kim DH, et al. The impact of microemulsion viscosity on oil recovery. In: SPE improved oil recovery symposium, Tulsa, Oklahoma; 2012. doi:10.2118/154275-MS.

Winsor PA. Solvent properties of amphiphilic compound. London: Butterworths Scientific Publications; 1985.